Eur. Phys. J. B **48**, 189–197 (2005)
DOI: 10.1140/epjb/e2005-00395-8

THE EUROPEAN
PHYSICAL JOURNAL B

Current-induced voltage oscillations in superconducting $Y_1Ba_2Cu_3O_{7-\delta}$

K. Kiliç, A. Kiliç[a], A. Altınkök, H. Yetiş, and O. Çetin

Abant Izzet Baysal University, Department of Physics, Turgut Gulez Research Laboratory, 14280 Bolu, Turkey

Received 13 June 2005 / Received in final form 5 October 2005
Published online 16 December 2005 –

Abstract. We investigated influence of bidirectional square wave current with long periods and dc current on the evolution of the voltage-time $(V-t)$ curves in superconducting polycrystalline bulk $Y_1Ba_2Cu_3O_{7-\delta}$ (YBCO) material at the temperatures near the critical temperature. In a well-defined range of amplitudes and periods of driving current, and temperatures, novel type of non-linear dynamic responses was observed by means of the $V-t$ curves. It was seen that such a non-linear response to bidirectional square wave current sometimes reflects itself as regular sinusoidal-like voltage oscillations. The sinusoidal-like and non-sinusoidal oscillations were discussed mainly in terms of the dynamic competition between pinning and depinning and significant relaxation effects which appear in this competing process. The density fluctuations associated with the current induced self-magnetic flux (SMF) lines and semi-elastic coupling of SMF lines with the pinning centers were also considered as possible physical mechanisms in the interpretation of the experimental results.

PACS. 74.72.Bk Y-based cuprates – 74.25.Qt Vortex lattices, flux pinning, flux creep

Introduction

The subject of current-induced organization of vortices have attracted much attention. The experimental [1–8] and theoretical studies [9,10], and many realistic computer simulations [11–27] show that the magnitude of current can induce an increase or decrease in the order of moving vortex configuration. The detailed investigations reveal that the degree of order of a vortex system mainly depends on the interaction between the vortices and pinning strength related to the disorder in material [3–8,28,29]. In one hand, the interaction of vortices maintains order, in the other hand, the pinning promotes disorder. As the vortices are set in motion with an external current, a motional reorganization in vortex configuration develops gradually depending on the magnitude of applied current. Such a vortex dynamics reflects itself as a low-frequency noise [29,30], slow voltage oscillations [3,4], history dependent dynamic response [31], memory effect, etc. [6,32]. A generic model which explains many interesting phenomena associated with such anomalous vortex dynamics has been proposed by Paltiel et al. [7]. In their experimental studies on a single crystalline sample of 2H-$NbSe_2$, these authors showed that the applied current flowing at the edges of the sample causes a contamination by injecting a disordered vortex phase, while the one flowing in the bulk acts as an annealing mechanism. In this competing process, the driving current serves as an effective temperature in the usual sense as in the statistical mechanics. This generic model could be also applied for the investigation of vortex dynamics in high temperature superconductors [33].

It has been shown that the dynamics of the vortices in type-II superconductors depends also on the type of the transport current modulations [3,4,30]. The experimental studies established that the direct current, alternating current such as square wave and asymmetrical square wave currents cause several implications [3,4,32]. For instance, it has been observed that high vortex mobility appears for alternating currents, but no apparent vortex motion for direct currents [3,32]. Henderson et al. [32] have investigated the vortex dynamics in a single crystalline sample of 2H-$NbSe_2$ by observing how the current driven ordering of moving state evolves when the driving current is changed. Such fast transport measurements performed by Henderson et al. [32] show that the response includes three distinct regimes depending on the type of current: no measurable voltage for a dc current, growing of voltage from zero voltage for a bidirectional square wave current, and a decay in voltage for a dc current. For a square wave current, this experiment shows nicely the current driven re-ordering of vortices since the response grows with every current reversal. More interestingly, the experiments performed by Gordeev et al. [3,4] reveal that the asymmetrical square wave currents cause slow voltage oscillations on long time scale in de-twinned single crystalline of $Y_1Ba_2Cu_3O_{7-\delta}$ sample. Such low frequency

[a] e-mail: kilic_a@ibu.edu.tr

oscillations were attributed to the structural feature in the vortex lattice crossing the sample together with the drifting vortices. A similar study on single crystalline sample of $Y_1Ba_2Cu_3O_{7-\delta}$ (YBCO) has been reported by Kwok et al. [30]. In that study, a dynamic instability just below the melting (or freezing) line corresponding to the material has been observed as a time oscillation to an ac sinusoidal type current.

The transport relaxation studies associated with the time evolution of sample voltage show that there are remarkable time effects in transport measurements, which deserve to be investigated [33,34]. Observing of the details of the vortex dynamics on short and long time scales together with the initial stage of the flux motion becomes possible via these measurements. The aim of the present study is to investigate the time evolution of voltage ($V - t$ curves) at low dissipation levels for different types of transport currents, such as dc current and bidirectional square wave current with long periods, in superconducting polycrystalline $Y_1Ba_2Cu_3O_{7-\delta}$ (YBCO) material. The measurements were carried out as a function of temperature (T), current (I), and the period (P_I) of bidirectional square wave current on both short and moderate time scales at zero magnetic field. It was observed that the regular sinusoidal type oscillations evolve in a well-defined range of amplitudes and periods of drive, and temperature. We interpreted the sinusoidal like and non- sinusoidal oscillations mainly in terms of a dynamic competition between pinning and depinning which causes prominent relaxation effects. The oscillating mode was also correlated to the defective flow of current induced self-magnetic flux (SMF) lines in a multiply connected network, and semi-elastic coupling of SMF lines with pinning centers.

Experiment

The YBCO sample has been prepared from the high purity powder of Y_2O_3, $BaCO_3$ and CuO by using the conventional solid state reaction. In order not to apply high currents and to reduce the possible heating effect which will occur at current leads, the sample for the transport measurements is shaped carefully in the dimensions of length $l \sim 4$ mm, width $w \sim 0.1$ m, thickness $d \sim 0.2$ mm. After the shaping of the sample, the four conductive pads are placed onto the sample by using silver paint and annealed ~1–2 h at 150 °C under O_2 atmosphere. The pure copper wires are attached by silver paint. The measured contact resistance by using the three point method is of order of $\sim 10^{-3}$ Ω below T_c and $\sim 10^{-2}$ Ω at room temperature. In this case, the power dissipated at the current contacts would be $\sim 6.5 \times 10^{-6}$ watt for a current of $I = 50$ mA, and, of course, this would have no dramatic effects on the evolution of $V - t$ curves. Transport measurements were carried out using standard four-point method, and performed in a closed cycle refrigerator [Oxford Instruments (OI) CCC1104]. In the experiments, Keithley-182 with a resolution 1 nV and Keithley-220 were used in measuring the sample voltage and applying the current, respectively. The temperature was recorded by a calibrated 27 Ohm Rhodium-Iron thermocouple (OI Calibration number 31202), and a temperature stability better than 10 mK were maintained during the experiments (OI, ITC-503 temperature controller) [33,34].

In this study, the time evolution of voltage ($V - t$ curves) was measured for a bidirectional square wave current with different amplitudes and long period (P_I) at zero field. We note that, for our purpose, the commercial current source Keithley-220 and Keithley-182 are quite relevant to form such bidirectional square wave currents with long periods and to read low voltage levels with large precision, respectively. The measured voltage is the average value of 5 readings for each data point. After the current is applied, just at this time, we start to measure the developing voltage across the sample as a function of time. Thus, monitoring of all details of the time evolution including the transient effects becomes available. In the experiments, in order to see the influence of dc current on the evolution of $V - t$ curves, the bidirectional current was switched to dc currents in the final stage of some of the measurements.

Experimental results

Figures 1a to 1d show the time evolution of sample voltage measured at $T = 85.5$ K for a bidirectional symmetric square wave (BSW) current with different amplitudes of 9, 11, 12, and 13 mA at zero magnetic field, respectively. The upper panels in Figure 1 represent the time variation of the driving current. The period (P_I) of the drive for each $V - t$ curve illustrated in Figure 1 is 20 s. The experimental $V - t$ curves consist of two different regimes. One of them is the development of a sharp increase in sample voltage during the first half cycle of BSW current; the other regime is characterized by nearly periodic sinusoidal-type oscillations of voltage in the remaining time scale of the experiment. These regular voltage oscillations in the $V - t$ curves appear after approximately one complete cycle of the driving BSW current (i.e., at around $t = 20$ s), and the period of the oscillations is nearly equal to the period of the drive. Another observation is the gradual increase in the amplitude of the oscillations as the amplitude of the driving current is increased from 9 to 12 mA. The amplitude of oscillations takes its highest value when the BSW amplitude is 12 mA, and the oscillations become more regular and more pronounced. Interestingly, increasing of the amplitude of driving current from $I = 12$ mA to 13 mA causes a marked decrease in amplitude of oscillations. This implies that, in a given temperature range, the amplitude of oscillations passes through a maximum for certain values of both the amplitude and period of BSW driving current. On the other hand, although the driving current is bidirectional the voltage oscillations in Figures 1a to 1d remain always positive. We also note that the oscillations develop on a time-independent background which increases slightly with the amplitude of bidirectional current. In addition, it seems that there is a phase difference between response and drive.

Figure 2 shows a long time evolution of the voltage over a time range from 0 to 600 s for BSW current with an

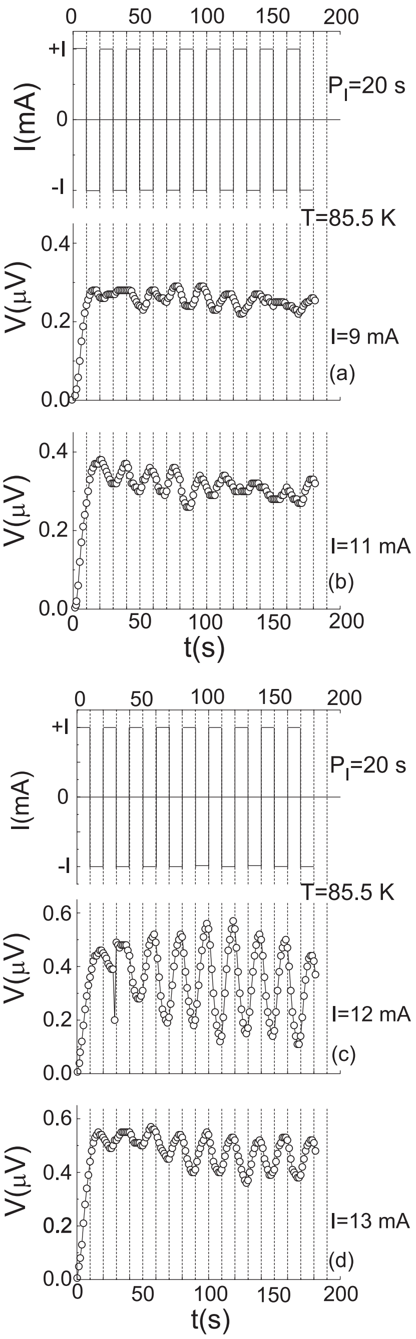

Fig. 1. Time evolution of the sample voltage measured at $T = 85.5$ K for a bidirectional symmetric square wave (BSW) current with different amplitudes of (a) $I = 9$ mA, (b) $I = 11$ mA, (c) $I = 12$ mA, and (b) $I = 13$ mA, respectively. The top panel represents BSW current with a period $P_\mathrm{I} = 20$ s.

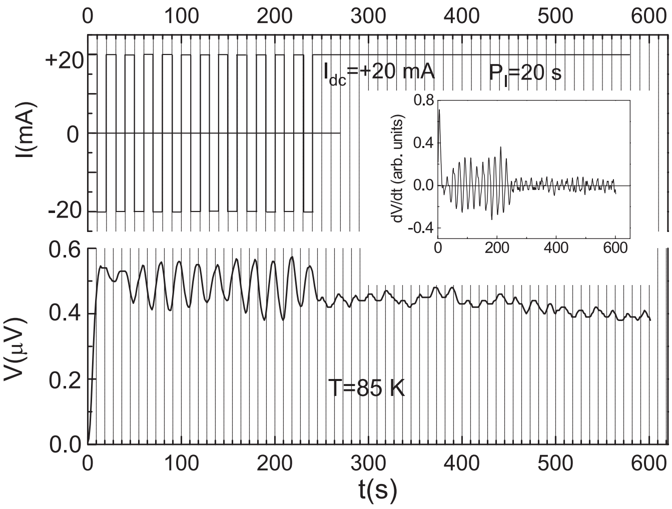

Fig. 2. Long time evolution of the sample voltage measured at $T = 85$ K for a BSW current with an amplitude of 20 mA and period of 20 s (upper panel). The driving current was switched to +20 mA dc current at around $t = 220$ s. The inset shows the time derivative of the sample voltage.

amplitude of 20 mA and a period of 20 s, until $t \sim 240$ s and a dc current of $I = +20$ mA for the rest of the experiment, which is illustrated in the upper panel. The measurement was carried out at $T = 85$ K. As in the case of Figure 1, the response evolves in two-stage: a sharp increase in voltage at the beginning of the measurement, and, periodic regular sinusoidal type oscillations of voltage after initial transient effects corresponding to nearly one period of the drive. In order to see the influence of the dc current on the evolution of voltage, at around $t = 240$ s, the BSW current was switched to +20 mA dc current for the rest of the relaxation process. After switching to dc current, the regular voltage oscillations disappeared and a relative decrease in the amplitude of measured voltage which is similar to a noise pattern was observed. To demonstrate better the sinusoidal-type oscillations and remove the background voltage in the experimental $V - t$ curve, we calculated the first derivative of the $V - t$ curve with respect to time and plotted it as an inset in Figure 2.

Figures 3a to 3d show the $V - t$ curves measured at $T = 81.5$ K for the BSW current with a period of 75 s and amplitude of 40, 45, 47 and 50 mA , respectively. The repetitive regular oscillations evolve after the first half period of driving current, where the polarity of the drive changes abruptly from positive to negative. Although the regular sinusoidal-type oscillations in Figure 3a appear, it is seen that gradual distortions in the oscillations become more pronounced as the amplitude of the applied current is increased, and, finally, the oscillations change into square wave-type. This process implies that the oscillations are quite sensitive to the magnitude of the driving current. Furthermore, the sample voltage seems in opposite phase with the drive for the current amplitudes of $I = 45$, 46, and 47 mA. However, it is seen from Figure 3d that the phase difference between the sample voltage and the drive disappears so that the sample voltage follows the drive. Note also that the responses in Figures 3c and 3d corresponding to the driving currents of 47 and 50 mA become different as compared to that of observed in $V - t$ curves for smaller currents: in these $V - t$ curves, the sample voltage takes positive and negative values so that a regular behavior which reflects the change of polarity of the driving current is observed despite the phase difference appearing in voltage response in Figure 3c. Another

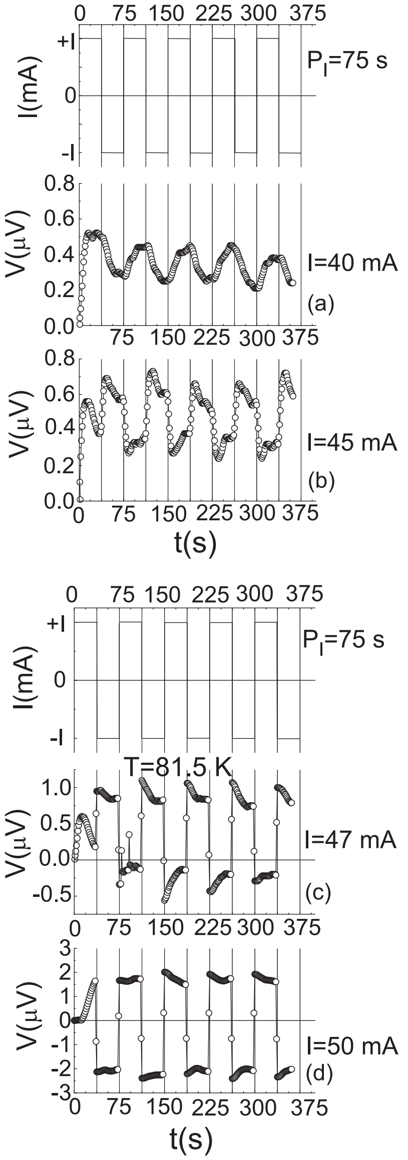

Fig. 3. Time evolution of the sample voltage measured at $T = 81.5$ K for BSW current with a period of 75 s and amplitude of (a) 40 mA, (b) 45 mA, (c) 47 mA, and (d) 50 mA. Upper panels show the time variation of the drive.

common feature of the $V - t$ curves shown in Figures 3b to 3d is that absolute value of the sample voltage tends to decrease or increase within the time intervals where the amplitude of driving current remains constant. In fact, it can be expected that BSW currents having long periods (75 s) cause relaxation effects in the $V - t$ curves. This finding indicates that the period of the driving current has a substantial effect on the evolution of $V - t$ curves.

Figures 4a to 4c show the $V - t$ curves measured at $T = 81.5$ K for a BSW current with amplitude of 45 mA and different periods of $P_I = 10$, 20 and 40 s, respectively. The measurements were carried out in a time interval of 0–360 s. As can be seen from the $V - t$ curves, regular sinusoidal-type oscillations appear as the period of the drive decreases. However, it is seen from Figure 4c that the period of drive of $P_I = 40$ s leads to re-appearance of the distortions in sample voltage, so that, for $P_I = 75$ s, the pronounced distortions in sample voltage were observed at the same current amplitude [see Fig. 3b]. Note that the sample voltage manifests itself as a decrease or increase in time against to the change of the polarity of the drive and tries to be in phase with it.

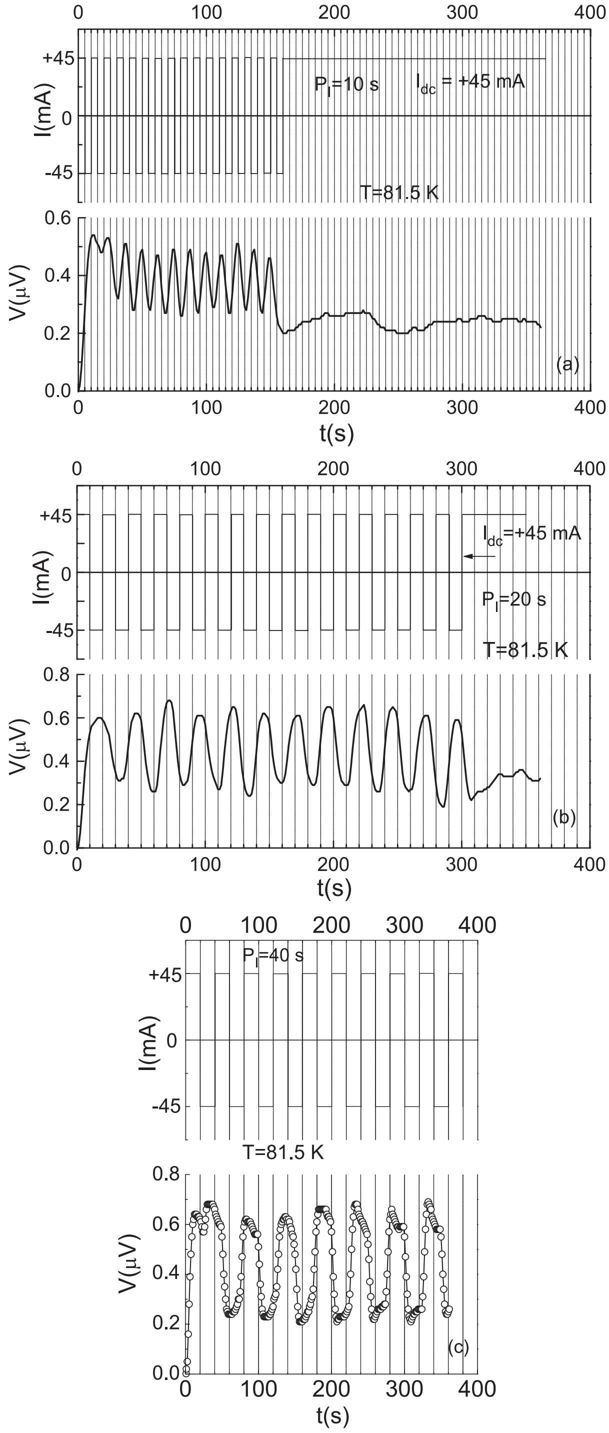

Fig. 4. Period dependence of the voltage oscillations at a constant amplitude of 45 mA at $T = 81.5$ K: (a) $P_I = 10$ s, (b) $P_I = 20$ s, (c) $P_I = 4$ s. The drive is switched to a dc current of +45 mA $t = 160$ and 320 s in Figures 4a and 4b, respectively.

To observe again the effect of dc current on the evolution of $V - t$ curves, the driving current was switched to +45 mA dc current at around $t = 160$ and 320 s, as is seen in Figure 4a and in Figure 4b, respectively. The sinusoidal-type oscillations disappear as the BSW current is switched to the dc current, and, then, a pattern similar to noise measurements is observed. Note that all of the experimental observations given in Figures 1–4 eliminate any possible artifact due to the experimental set-up.

Discussion

To better describe the $V - t$ curves represented above, we suggest that the voltage developing across the sample arises from the motion of the self-magnetic flux lines induced by the transport current. The self-magnetic field B_s induced by the applied transport current can be calculated by using the Maxwell equations. For a sample in the shape of the rectangular prism, B_s becomes equal to $\mu_0\gamma J$, where μ_0 is the permeability of free space ($\mu_0 = 4\pi\times10^{-7}$ H/m), γ is the geometric parameter of the sample and given as $\gamma = wd/2(w + d)$, w is the width, d is the thickness of the sample [35–40]. The slab considered for the transport measurements was in dimensions of length $l \sim 4$ mm, width $w \sim 0.1$ mm, and thickness $d \sim 0.2$ mm. Thus, the self-field is found as ~0.2 mT for a transport current of 45 mA. It may be suggested that the transport current values used in our measurements (or the self-magnetic field induced by the transport current) are sufficiently weak to suppress the superconducting order parameter. Besides, the order of the voltage (~10^{-7}–10^{-6} V) recorded in the present measurements is in favor of this idea. We note that the flux lines associated with the self-field of the transport current are mainly concentrated in the intergranular region. This description shows that the time effects in $V - t$ curves originate essentially from the intergranular region where the dynamics of the Josephson vortices develops.

We now focus on sharp increase in sample voltage at the beginning of the measurement observed in all $V - t$ curves before the voltage oscillations are set in. In this stage, the self-magnetic flux (SMF) lines induced by the transport current are subject to, mainly, two competing processes, pinning and de-pinning: it is quite natural to expect that the competition between them can be very complex and can strongly depend on the temperature, external magnetic field, current and also the chemical and anisotropic states of the sample, the structure of the multiply connected weak link network etc. Thus, different flow patterns inside the sample may develop depending on the strength of this competition [6,8,33]. In this case, the sharp increase in sample voltage can be evaluated that the pinning and de-pinning work together and simultaneously during the flux motion. However, after the transient effects, the process develops in favor of de-pinning when there is an increase in sample voltage. In the final stage, the response manifests itself as voltage oscillations evolving in sinusoidal-like or non-sinusoidal types, which follow generally the period of the driving current.

Of course, the first question here is whether the repetitive voltage oscillations, in particular, sinusoidal-like oscillations, represent fundamentally a new kind of flux dynamics induced by the driving current or not. Let us first discuss the origin of the nature of the oscillations appearing due to the bidirectional square wave current.

In the noise measurements carried out on a detwinned YBCO single crystal below the melting transition by D'anna et al. [29], the origin of the voltage oscillations was attributed to the surface barrier which influences the coherent motion of the vortices entering or leaving through the large faces of the crystal. Gordeev et al. [3,4] showed that an asymmetric square wave current causes low-frequency periodic voltage oscillations in detwinned single crystal of YBCO sample below the vortex lattice melting temperature in the presence of an external magnetic field, i.e., $H = 2$ T. They reported that the temporal asymmetry in square wave current and its periodic reversal are essential to observe such regular oscillations. Further, they attributed the regular oscillations to the transit of periodic vortex density fluctuations which is similar to the dynamics of the charge density waves (CDWs) driven by a sufficiently large driving force [41–55]. In a study, Kwok et al. [30] attributed the observation of the oscillatory instability in single crystal YBCO sample to the strong competition between the driving and pinning forces and correlated it to the elasticity of the vortex solid and the long time relaxation effects.

In our case, the experimental results show that the presence of regular sinusoidal-like voltage oscillations depends strongly on the magnitude of amplitude of BSW current and also its period at a given temperature range. Such type of coherent oscillations could be also observed for other temperature ranges provided that the period and amplitude of the driving current are well defined. The coherent oscillations in Figures 1, 2, 3a, 4 suggest that the majority of SMF lines which are in motion drifts slowly and tries to traverse the sample, but, does not entirely leave it. In this case, the SMF lines remain in an oscillating mode and move forth and back, that is easily resolved in our experiments. At this point, it is necessary to recall the role and importance of the pinning on the evolution of $V - t$ curves, since the type of pinning centers and the pinning strength determine the flow pattern of flux lines evolving inside the sample. We suggest that the regular sinusoidal type oscillations arise from a strong dynamic competition between pinning and depinning process [30]. This is one of the main reasons why the regularities or distortions appeared in the evolution of some of the $V - t$ curves show a strong dependence on the period and magnitude of the driving current. In one hand, the interplay between pinning and depinning can determine the dynamics evolving in the intergranular region, in the other hand, inhomogeneous distribution of SMF lines, the short and long range dynamic correlations between them can play another important role in the evolution of the oscillations. In addition, the regular sinusoidal-type oscillations suggest that the interaction between SMF lines and pinning centers could be semi-elastic coupling rather than elastic. In this description, the oscillating mode can be closely related to the defective flow of SMF lines in which some of them are moving and the others remain pinned i.e., non-uniform flux motion [3,4,32,33]. Such a flow pattern is a prominent feature of plastic regime [11,16,18, 21,32–34]. Many realistic computer simulations revealed that, at low currents (or at low driving force), the vortex lattice becomes highly defective and exhibits several different plastic flow regimes due to the pinning strength. For instance, in a study, Olson et al. [18] showed the presence of the regime of semi-elastic flow due to the pinning strength by using large-scale molecular dynamic simulations. Their study gave a measurable voltage noise spectrum which could be changed by adjusting the degree of the dynamic competition between pinning and de-pinning. Further, we also consider that the relaxation effects which become more significant, in particular, at large period of BSW current (see, for instance, Fig. 3) have a determining property on the observation of the oscillations. Indeed, at long periods and large amplitude of the drive, the competition between pinning and depinning reflects itself as significant relaxation effects related to voltage decays, which correspond to a decrease or increase in sample voltage (see, for instance, Figs. 3b–3d). This indicates that the moving entity explores new accessible states and tries to go to a new equilibrium state in time during the positive or negative part of BSW current.

One of the interesting observations seen in $V-t$ curves given in Figures 1a to 1d, Figures 2, 3a to 3b, and Figures 4a to 4c is that the voltage oscillations remain positive despite the fact that the driving current is bidirectional. Here, the bidirectional self field induced by the BSW current can be assumed one of the main reasons to explain the regular voltage oscillations. It is naturally expected that, when the polarity of the driving current changes, the direction of the SMF lines would change too, in addition, the voltage developing in the direction of the current would follow the polarity change. As can be seen from these figures, during the time corresponding to the positive part of the driving current, the dissipation increases non-linearly and reaches nearly a value where the oscillations ride on top a time independent of voltage value. When the current becomes negative, due to the spatial reorganization of the SMF lines resulting from the dynamic competition between pinning and depinning together with the relaxation effects, the dissipation can not return back zero or can not find enough time to take a negative value, whereas, such a physical case is observed relatively at large values of the bidirectional current as in Figures 3c and 3d.

Within this description, the measured voltage value can be written simply as the sum of two terms: $V(t) = V_0 \pm \delta V(t)$, where V_0 is the time independent background voltage value and $\delta V(t)$ is the time dependent part. Here, "$\pm$" sign means that the oscillating term can be positive or negative depending on the polarity change of BSW current. Without background voltage value, or if $V_0 < \pm\delta V(t)$, then the oscillating term will dominate the dissipation and the measured voltage will be $V(t) > 0$ or $V(t) < 0$ for the positive or negative part of the BSW current, respectively. As can be seen from $V-t$ curve given in Figure 1d, the average amplitude of oscillations is about 0.15 μV (this value is $\sim$0.2 μV in the studies by Gordeev et al. [3] and Kwok et al. [30]) and it is less than the background voltage value of $\sim$0.5 μV. Thus, the voltage oscillations can remain positive despite the fact that the driving current is bidirectional. However, when the dissipation reaches or exceeds $\sim$1 μV, as is seen in Figures 3c and 3d, the voltage oscillations shift from positive to negative region. In parallel to this, the background voltage value disappears as the amplitude of BSW current is large enough (see Fig. 3d) and the measured voltage reflects directly the effect of bidirectional current by taking positive and negative values.

We believe that appearance or disappearance of the phase difference between the response and the BSW drive originates from the dynamic competition between pinning and depinning and also from the strong diamagnetic response of the sample to the drive in a complicated way. In addition, the amplitude of the BSW current has a direct contribution to the evolution of the phase difference seen in $V-t$ curves. At low dissipation levels, the moving entity does not respond immediately to the drive, since pinning is effective and dominates the motion of SMF lines, and, thus, a delay which causes a phase difference between the response and drive appears. However, the phase difference observed in $V-t$ curves disappears when the large enough BSW current amplitude is applied as in Figures 3c and 3d.

We note that the motion of SMF lines develops in the intergranular region where the local superconducting order parameter is strongly suppressed since the grains have superconducting properties better than that of weak link structure. The flux motion in this region is controlled by the structural disorder, distribution of the pinning centers, intrinsic character of grain boundaries and misorientation angle between the adjacent grains, etc., and, the dynamic competition between pinning and depinning together with the disorder in the coupling strength between the superconducting grains (i.e. Josephson coupling effects) determine effectively the magnitude of the observed dissipation [56]. When the effective field (or self-field due to the transport current) reaches the Josephson decoupling field, the weakly coupled grains through Josephson interaction become decoupled by causing a dissipation. In this description, as the measured dissipation is considered, the experimental result shown in Figure 3d can be considered as an indication of decoupled superconducting grains. Thus, the motion of the SMF lines in the junction network where the weak pinning regime exists becomes relatively correlated and the measured voltage is that of the normal-conducting grain boundaries. In addition, we note that the regular sinusoidal type voltage oscillations disappear when the superconducting grains with different order parameters remain independent of each other despite some proximity effect due to the presence of the low-angle boundaries which give strong coupling.

In our measurements, the response generally oscillates with the period of BSW drive. The Fast Fourier Transform (FFT) of the corresponding $V-t$ curve can be taken to determine the spectral content of the oscillations. A typical example concerning the FFT of the $V-t$ data given in Figures 4a to 4c is illustrated in Figures 5a to 5c, respectively. FFT shows that there is a fundamental frequency accompanied by its harmonics. The fundamental periods ($P_{V,FFT}$) of oscillations found from the FFT of Figures 4a to 4c are 11.7, 23.4, and 46.5 s, respectively. Note that the values of $P_{V,FFT}$ are comparable to actual corresponding BSW, i.e., $P_I = 10$, 20 and 40 s. This finding suggests the presence of a dynamic physical case, which resembles the driven CDWs by an external drive. It has been already argued by Gordeev et al. [3] that the system of weakly pinned vortices is similar to the pinned CDW state. Experimental studies on CDW revealed that, in a current or voltage controlled experiment, coherent voltage or coherent current oscillations appear across the sample after a threshold value of the driving current or voltage [43,45,52,54]. In addition, it has been shown that the sliding CDW can cause coherent oscillations at well defined frequencies of the drive [46–48]. Furthermore, it is well known that CDW's are characterized by an order parameter which has an amplitude and a phase [50,55]. A phenomenological theory, which considers an order parameter correlated to the superconducting state, was proposed by Ginsburg and Landau a few decades ago, i.e, GL theory [57]. Both the GL theory and its extended versions, such as time dependent GL theory, predict the spatial and time variation of the order parameter which are in reasonable agreement with the physical expectations [57]. In addition, GL theory provides a relation between the current carrying capacity of the sample and the order parameter. It seems that there are some similarities between description of the superconductivity and the driven CDW's. Therefore, on the basis of these similarities as a first approximation, we suggest that a physical mechanism concerning the density fluctuations of SMF lines can be introduced. Such coherent density fluctuations in the sample can develop and can do a similar effect as in the case of the CDW's.

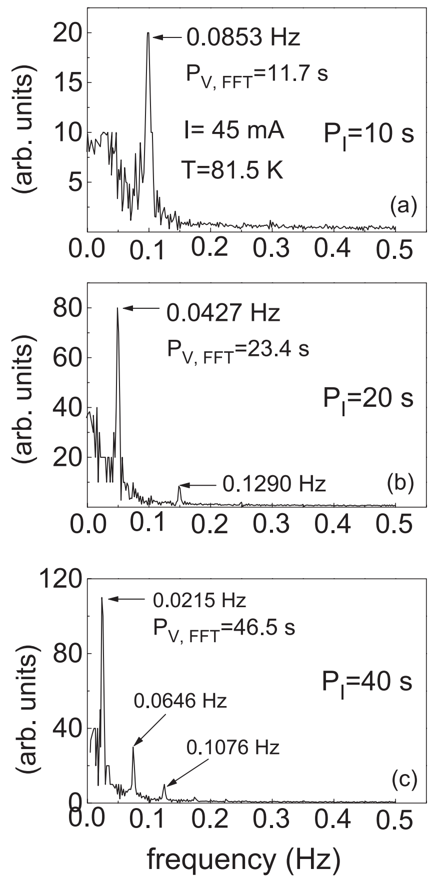

Fig. 5. Fast Fourier Transform (FFT) of the $V - t$ curves given in Figures 4a to 4c measured at 81.5 K for BSW drive with amplitude of 45 mA and period of 10, 20, and 40 s, respectively. The fundamental frequencies and also their harmonics are marked on the curves. The fundamental periods $P_{V,FFT}$ found from FFTs is also given along with the periods of BSW current.

As is well known, the real structure of a superconductor is not perfect, variation in pin size, spacing, composition, and concentration can be expected. The granular HTSC materials consist of randomly oriented superconducting grains in which the grain boundaries act as Josephson weak links. In these materials, microcracks, anisotropy, compositional variations and residual stresses arising from the lack of oxygenation at the grain boundaries can be considered as the source of weak links, and, further, the junctions are highly ramified, not independent of each other and extends over the whole sample. Because of the short coherence length associated with the HTSCs, these materials usually sensitive to structural imperfections and the superconductivity in the intergranular region is much more sensitive to small scale structural or chemical imperfections as compared to intragrain region [56,59]. The coherence length sets the length scale variation of the superconducting order parameter by allowing a considerable suppression of the superconducting order parameter near the grain boundaries even in the presence of a weak external magnetic field. Low-field magnetization measurements support that the source of the irreversibility effects in the intergranular region is the flux trapping in the junction network [56,59]. Random distribution of inhomogeneities and the pinning effect require an inhomogenous distribution of the SMF lines together with different velocities which are not unique. The spatial variation in SMF lines along the intergranular region having the weak coupling strength can cause a considerable local suppression in the superconducting order parameter in different magnitudes. Thus, the appearance of the voltage oscillations can be assumed as a measure of time variation of the effective superconducting order parameter at grain boundaries. It can be concluded that any local variation in SMF lines over time corresponds to an increase or decrease in the suppression of the order parameter.

The experimental results reveal that a change in the polarity of the driving current is essential for establishing the regular voltage oscillations, as in the study of Gordeev et al. [3,4] This requirement is underlined clearly in the $V-t$ curves given in the inset of Figure 2 and also in Figures 4a and 4b, where the BSW current is switched to dc current. In these figures, switching to dc current causes relatively a decrease in the background of the sample voltage together with the disappearance of the voltage oscillations. This finding is an evidence for another physical effect of BSW current on the evolution of $V-t$ curves: the symmetric forwards and backwards oscillations of the driving current lead to increase in the measured voltage by facilitating the formation and growth of easy motion flow channels for SMF lines inside the sample. The SMF lines in this state being locally ordered and weakly pinned depin through such easy motion channels which evolve gradually [32]. A similar observation was also reported by Gordeev et al. [3]. These authors showed that asymmetric square wave currents result in higher voltage amplitudes with reduced low noise levels in detwinned YBCO crystals below the vortex-lattice melting temperature, while, a dc current induces highly non-uniform vortex motion.

Our experiments reveal that, in order to obtain regular voltage oscillations, the applied driving current should not exceed the effective Josephson critical current which depends strongly on the features of the random weak-link network and also on the temperature and external magnetic field [33]. The importance of this requirement is established well in Figure 3: a comparison between the $V-t$ curves in Figures 3a and 3b reveals that a slight increase in the amplitude of the driving current causes a considerable departure from the regular sinusoidal-type voltage oscillations and a further increase in amplitude of driving current causes completely their disappearance by destroying the semi-elastic coupling between SMF lines and pinning centers and leads relatively to a correlated flux motion. These experimental observations stress the fact that the magnitude of driving current with respect to effective Josephson critical current has a crucial role in obtaining regular sinusoidal-type voltage oscillations. Nevertheless, the current-induced distortions in oscillations can be avoided by adjusting the period of driving current. For instance, the distortions seen in the $V-t$ curve measured for BSW current with amplitude of 45 mA and period $P_{\text{I}} = 75$ s (Fig. 3b) disappear in Figures 4a–4c for $P_I = 10$, 20, and 40 s. This shows that the regular sinusoidal-type oscillations depend not only on the amplitude of driving current, but also on the period of the drive. All experimental observations presented above show the presence of current-induced re-organization of the SMF lines in the intergranular region.

Finally, we discuss the type of the vortices which take place in current-induced voltage oscillations. For HTSCs, it is commonly accepted that the Josephson vortices can be naturally generated in the weak-link structure of the granular material, and, even in single crystals, the vortices lying between Cu-O layers are in Josephson character [9,10,33,34,40,59,60]. In addition, it is well known that, inside the superconducting grains, the vortices evolve in the form of Abrikosov — type vortices. We suggest that the voltage oscillations and also the time effects observed in $V-t$ curves measured in this study originate effectively from the intergranular region and, thus, should reflect naturally the oscillations of the flux lines which are of Josephson-type. Our studies on transport relaxation measurements give a further support for this suggestion [33,34].

Conclusion

In this paper, we investigated the influence of the bidirectional square wave (BSW), and dc currents on the evolution of the voltage-time ($V-t$) curves in superconducting polycrystalline bulk $Y_1Ba_2Cu_3O_{7-\delta}$ (YBCO) material at the temperatures near the critical temperature at zero magnetic field. It was found that a non-linear response seen in $V-t$ curves to the bidirectional driving current with sufficiently short periods or sufficiently low amplitude reflects itself as regular sinusoidal-type voltage oscillations, when the bidirectional current was switched to dc current, however, the oscillations disappear immediately. The regular sinusoidal- or non sinusoidal-type voltage oscillations were interpreted in terms of the defective flow of current-induced self-magnetic flux (SMF) lines in a multiply connected net work, and semi-elastic coupling between SMF lines and pinning centers. Furthermore, it was shown that the voltage oscillations depend strongly on the amplitude and period of BSW current on both short- and long-time scales. In addition, we found that a change in the polarity of driving current is essential in observing of such oscillations. Finally, we conclude that the sinusoidal-type voltage oscillations reflect the oscillations of the flux lines which are of Josephson-type.

The authors would like to thank Prof. Dr. M. Cankurtaran at Hacettepe University for valuable discussions.

References

1. S. Bhattacharya, M.J. Higgins, Phys. Rev. Lett. **70**, 2617 (1993)
2. S. Bhattacharya, M.J. Higgins, Phys. Rev. B **49**, 10 005 (1995)
3. S.N. Gordeev, P.A.J. de Groot, M. Oussena, A.V. Volkozup, S. Pinfold, R. Langan, R. Gagnon, L. Taillefer, Nature **385**, 324 (1997)
4. S.N. Gordeev, P.A.J. de Groot, M. Oussena, R.M. Langan, A.P. Rassau, R. Gagnon, L. Taillefer, Physica C **282**, 2033 (1997)
5. M.C. Hellerqvist, A. Kapitulnik, Phys. Rev. B **56**, 5521 (1997)
6. Z.L. Xiao, E.Y. Andrei, M.J. Higgins, Phys. Rev. Lett. **83**, 1664 (1999)
7. Y. Paltiel, E. Zeldov, Y.N. Myasoedov, H. Shtrikman, S. Bhattacharya, M.J. Higgins, Z.L. Xiao, P.L. Gammel, D.J. Bishop, Nature **403**, 398 (2000)
8. Z.L. Xiao, E.Y. Andrei, P. Shuk, M. Greenblatt, Phys. Rev. Lett. **86**, 2431 (2001)
9. G. Blatter, M.V. Feigel'man, V.B. Geshkenbein, A.I. Larkin, V.M. Vinokur, Rev. Mod. Phys. **66**, 1125 (1994)
10. E.H. Brandt, Rep. Prog. Phys. **58**, 1465 (1995)
11. A.-C Shi, A.J. Berlinsky, Phys. Rev. Lett. **67**, 1926 (1991)
12. A.E. Koshelev, V.M. Vinokur, Phys. Rev. Lett. **73**, 3580 (1994)
13. R.A. Richardson, O. Pla, F. Nori, Phys. Rev. Lett. **72**, 1268 (1994)

14. C. Reichhardt, C.J. Olson, J. Groth, S. Field, F. Nori, Phys. Rev. B **52**, 10 441 (1995)
15. C. Reichhardt, C.J. Olson, J. Groth, S. Field, F. Nori, Phys. Rev. B **52**, R8898 (1996)
16. C. Reichhardt, J. Groth, C.J. Olson, S.B. Field, F. Nori, Phys. Rev. B **54**, 16108 (1996)
17. C. Reichhardt, J. Groth, C.J. Olson, S.B. Field, F. Nori, Phys. Rev. B **56**, 14196 (1997)
18. C.J. Olson, C. Reichhardt, J. Groth, S.B. Field, F. Nori, Physica C **290**, 89 (1997)
19. C.J. Olson, C. Reichhardt, F. Nori, Phys. Rev. B **56**, 6175 (1997)
20. C. Reichhardt, C.J. Olson, F. Nori, Phys. Rev. B **57**, 7937 (1998)
21. C.J. Olson, C. Reichhardt, F. Nori, Phys. Rev. Lett. **81**, 3757 (1998)
22. C. Reichhardt, C.J. Olson, F. Nori, Phys. Rev. B **58**, 6534 (1998)
23. C. Reichhardt, C.J. Olson, F. Nori, Phys. Rev. Lett. **78**, 2648 (1997)
24. C.J. Olson, C. Reichhardt, F. Nori, Phys. Rev. Lett. **80**, 2197 (1998)
25. C. Reichhardt, F. Nori, Phys. Rev. Lett. **82**, 414 (1999)
26. A.P. Mehta, C.J. Olson, C. Reichhardt, F. Nori, Phys. Rev. Lett. **82**, 3641 (1999)
27. Y. Cao, Z. Jiao, H. Ying, Phys. Rev. B **62**, 4163 (2000)
28. A.C. Marley, M.J. Higgins, S. Bhattacharya, Phys. Rev. Lett. **74**, 3029 (1995)
29. G. D'Anna. P.L. Gammel, H. Safar, G.B. Alers, D.J. Bishop, Phys. Rev. Lett. **75**, 3521 (1995)
30. W.K. Kwok, G.W. Craptree, J.A. Fendrich, L.M. Paulius, Physica C **293**, 111 (1997)
31. W. Henderson, E.Y. Andrei, M.J. Higgins, S. Bhattacharya, Phys. Rev. Lett. **77**, 2077 (1996)
32. W. Henderson, E.Y. Andrei, M.J. Higgins, Phys. Rev. Lett. **81**, 2352 (1998)
33. A. Kiliç, K. Kiliç, O. Çetin, J. Appl. Phys. **93**, 448 (2003); Virtual J. Appl. Supercon. **4**, 1 (2003)
34. K. Kiliç, A. Kiliç, H. Yetiş, O. Çetin, Phys. Rev. B **68**, 144513 (2003); Virtual J. Appl. Supercon. **5**, 8 (2003)
35. R.B. Stephens, Cryogenics **29**, 399 (1989)
36. H. Kliem, A. Weyers, J. Lützner, J. Appl. Phys. **63**, 1534 (1990)
37. A. Kilic, Supercond. Sci. Technol. **8**, 497 (1995)
38. T. Henning, H. Kliem, A Weyers, B. Bauhofer, Supercond. Sci. Technol. **10**, 721 (1997)
39. A. Kiliç, K. Kiliç, S. Senoussi, K. Demir, Physica C **294**, 203 (1998)
40. A. Kiliç, K. Kiliç, S. Senoussi, J. Appl. Phys. **84**, 3254 (1998)
41. H. Fukuyama, P.L. Lee, Phys. Rev. B **17**, 535 (1978)
42. R.M. Fleming, C.C. Grimes, Phys. Rev. Lett. **42**, 1423 (1979)
43. J. Dumas, C. Schlenker, J. Markus, R. Buder, Phys. Rev. Lett. **50**, 757 (1983)
44. L. Pietronero, S. Strassler, Phys. Rev. B **28**, 5863 (1983)
45. R.P. Hall, A. Zettl, Phys. Rev. B **30**, 2279 (1984)
46. H.F. Hundley, A. Zettl, Phys. Rev. B **33**, 2883 (1986)
47. R.M. Fleming, L.F. Schneemeyer, Phys. Rev. B **33**, 2930 (1986)
48. S.N. Coppersmith, P.B. Littlewood, Phys. Rev. B **36**, 311 (1987)
49. G. Grüner, Rev. Mod. Phys. **60**, 1129 (1988)
50. S.N. Coppersmith, Phys. Rev. Lett. **65**, 1044 (1990)
51. S.N. Coppersmith, Phys. Rev. B **44**, 2887 (1991)
52. S.N. Coppersmith, A.J. Millis, Phys. Rev. B **44**, 7799 (1991)
53. M.R. Sarkardei, R.L. Jacops, Phys. Rev. E **51**, 1929 (1995)
54. K.L. Ringland, A.C. Finnefrock, Y. Li, J.D. Brock, S.G. Lemay, R.E. Thorne, Phys. Rev. Lett. **82**, 1923 (1999)
55. M. Karttunen, M. Haataja, K.R. Elder, M. Grant, Phys. Rev. Lett. **83**, 3518 (1999)
56. M. Tinkham, C.J. Lobb, Solid State Phys. **42**, 91 (1989)
57. V.L. Ginzburg, L.D. Landau, Zh. Eksperim. Theor. Fiz. **20**, 1064 (1950)
58. M. Thinkham, *Introduction to Superconductivity*, 2nd edn. (McGraw-Hill Inc), p. 319 (1996)
59. S. Senoussi, J. Phys. France III **2**, 1041 (1992)
60. A. Kiliç, K. Kiliç, O. Çetin, Physica C **384**, 321 (2003)